Competing structures in two-dimensional trapped dipolar gases

Barbara Gränz,[1] Sergey E. Korshunov,[2] Vadim B. Geshkenbein,[1] and Gianni Blatter[1]

[1]*Theoretische Physik, ETH Zurich, CH-8093 Zurich, Switzerland*
[2]*L.D. Landau Institute for Theoretical Physics, 142432 Chernogolovka, Russia*

We study a system of dipolar molecules confined in a two-dimensional trap and subject to an optical square lattice. The repulsive long-range dipolar interaction D/r^3 favors an equilateral triangular arrangement of the molecules, which competes against the square symmetry of the underlying optical lattice with lattice constant b and amplitude V. We find the minimal-energy states at the commensurate density $n = 1/b^2$ and establish the complete square-to-triangular transformation pathway of the lattice with decreasing V involving period-doubled, solitonic, and distorted-triangular configurations.

Competing structures and effects of commensuration appear in numerous physical systems. Prominent examples are atoms on surfaces, e.g., Krypton on graphite [1], vortices in modulated superconducting films [2], in periodic pinning arrays [3], and in a BEC subject to an optical lattice [4], flux quanta in Josephson junction arrays [5], or colloidal monolayers on periodic substrates [6]. A new realization of this physics is accomplished by assembling cold dipolar molecules [7] (e.g., KRb [8] or RbCs [9]) in a two-dimensional (2D) optical trap and stabilizing them with the help of a perpendicular electric field [10]. Adding a square optical lattice provides an effective substrate potential which competes against the triangular lattice arrangement favored by the long-range repulsive dipolar interaction. As a result, the system is expected to exhibit a variety of different configurations as a function of particle density and strength of the substrate potential. In this Rapid Communication, we find the minimal-energy states at commensurate density in the absence of quantum and thermal fluctuations and thereby establish the complete transformation pathway from the square to the triangular lattice. Contrary to previous studies, the cold molecule system, besides being clean, can be continuously tuned through various configurations by changing system parameters such as particle density and substrate potential amplitude. Even more, modifying the orientation or number of lasers, the symmetry of the optical lattice can be changed.

In the simplest case, the transformation pathway between lattices with different symmetries may involve a sequence of other uniform lattices. An interesting situation arises when new topological objects show up in intermediate *nonuniform* phases. The original "misfit problem" between a particle lattice with lattice constant a and a periodic substrate with incommensurate periodicity $b \neq a$ has first been formulated in one dimension (1D); these studies [11,12] have shown that the locked system at large potential V (with particle separation b) smoothly transforms into the free lattice (with separation a between particles) at $V = 0$ via a nonuniform soliton phase, with soliton cores approximating the free phase separating regions of locked phase. The commensurate-incommensurate transition in the 2D analog has been addressed by Pokrovsky and Talapov [13–15]; within their "resonance approximation," the problem reduces to a 1D one and the system develops a secondary structure in the form of a soliton-line array.

Going beyond the resonance approximation, we find that the square-to-triangular transformation in the dipolar system involves three separate transitions related to the formation of a period-doubled zigzag lattice as well as two instabilities towards nonuniform soliton phases (see Fig. 1).

We consider a 2D-confined molecular gas with dipolar interaction D/r^3 between the molecules,

$$E^{\text{int}} = \frac{1}{2} \sum_{i \neq j} \frac{D}{r_{ij}^3}, \qquad (1)$$

subject to an optical (substrate) lattice

$$E^{\text{sub}} = \frac{V}{2} \sum_{i,\alpha} [1 - \cos(\mathbf{q}_\alpha \cdot \mathbf{r}_i)]. \qquad (2)$$

The particles with density $n = 1/b^2$ equal to commensurate filling (one particle per minimum) are located at positions $\mathbf{r}_i$ with distances $r_{ij} \equiv |\mathbf{r}_i - \mathbf{r}_j|$; the substrate potential involves two modes $\mathbf{q}_1 = (q,0)$ and $\mathbf{q}_2 = (0,q)$ with $q = 2\pi/b$. Starting with the system's energy for N particles trapped within the area A, $E(A,N) = E^{\text{int}} + E^{\text{sub}}$, our task is to minimize the Gibbs free energy per particle

$$g(p) = G(A,N)/N = [E(A,N) + pA]/N, \qquad (3)$$

where the thermodynamic limit with fixed density $n = N/A$ is implied. We choose to work at fixed pressure p rather than fixed chemical potential, as this seems a better approximation to the experimental setup where molecules are confined to a trap. At $V = 0$, the molecules arrange in an equilateral triangular lattice with a lattice constant $a = (4/3)^{1/4}b > b$ and height $h = (3/4)^{1/2}a < b$; the resulting misfit parameter then is $s = b/h - 1 \approx 0.0746$. Given the purely repulsive interaction between molecules, the density n is related to the pressure $p = (3/2)ne_\triangle$, with $e_\triangle = e_\triangle^{\text{int}} \approx 4.446e_D$ the interaction energy per particle in the triangular lattice and $e_D = D/b^3$ the dipolar energy (the prefactor is conveniently calculated with an Ewald summation technique [16]). Upon switching on a small but finite potential $V > 0$, the rigid lattice assumes an energy $g_\triangle(V) = e_\triangle(V) + p/n \approx 11.115e_D + V$, increasing with amplitude V as each substrate mode contributes with an average $V/2$ to the energy. For a large potential V, the molecules arrange in a square lattice with lattice constant $b < a$ and an energy $g_\square \approx 11.186\,e_D$ independent of V as all particles
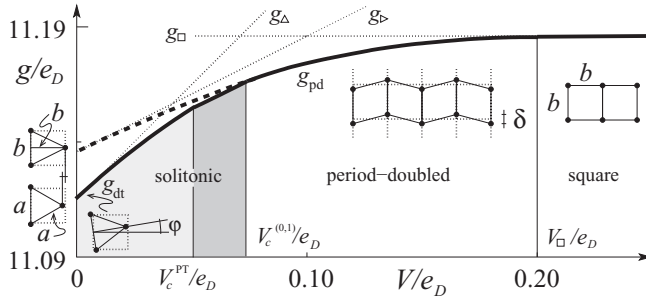
FIG. 1. Gibbs free energy of optimal states (thick line), triangular at $V = 0$, distorted and rotated triangular (g_{dt}) at small V, solitonic and period-doubled (g_{pd}) at intermediate V, and square for $V > V_\square$. Below the critical potential $V_c^{(0,1)}$, the period-doubled phase smoothly transforms into the triangular lattice via two soliton transitions involving different soliton arrays. The dashed line extrapolates the energy g_{pd} of the period-doubled phase. Dotted lines are energies of rigid triangular ($\triangle$), isosceles ($\triangleright$), and square ($\square$) configurations.

occupy potential minima. Besides the triangular and fully locked square lattices, a third low-energy configuration [17] is that of an isosceles triangular lattice (below called the *bb* lattice) with base b and a height b locked to one substrate mode (we have to break the symmetry and choose the mode along x) with an energy $g_{\triangleright}(V) = 11.136e_D + V/2$. The above expressions for $g_{\triangle}(V)$, $g_{\triangleright}(V)$, and $g_\square$ already provide a reasonable approximation to the energy g versus potential V diagram as illustrated in Fig. 1 (dotted lines).

Next, we account for deviations $\mathbf{u}_i$ of the particle coordinates $\mathbf{r}_i = \mathbf{R}_i^{latt} + \mathbf{u}_i$ from regular lattice positions $\mathbf{R}_i^{latt}$. Expanding Eq. (1) in the displacement field $\mathbf{u}_i$, the energy $g = g_{latt} + \delta g$ picks up a term

$$\delta g^{int} \approx \frac{1}{2N} \sum_{i,j} \mathbf{u}_i^T \, \hat{\Phi}^D\big(\mathbf{R}_{ij}^{latt}\big) \, \mathbf{u}_j, \tag{4}$$

with the elastic matrix $\hat{\Phi}^D(\mathbf{R}_{ij}^{latt})$ depending on the chosen lattice; the substrate potential contributes a second term δe^{sub} to δg, $\delta g = \delta g^{int} + \delta e^{sub}$.

For a large substrate potential V, the substrate enforces a square lattice with particle positions $\mathbf{R}_i^{latt} = \mathbf{R}_i^\square$. Since the true configuration at $V = 0$ is the triangular one, the square lattice becomes unstable when decreasing V. The symmetry-breaking instability is towards a period-doubled zigzag phase [18] and is conveniently analyzed in Fourier space; the elastic matrix $\hat{\Phi}^D(\mathbf{k})$ exhibits negative eigenvalues, with the most negative one $\phi_X^\perp = -3.958e_D n$ located at the X point $(\pi/b,0)$ of the Brillouin zone and describing a shear distortion [alternatively, the symmetry breaking involves the point $(0,\pi/b)$]. The contribution δe^{sub} shifts all eigenvalues by $Vq^2/2$, thus stabilizing the square lattice. The instability occurs when the first eigenvalue crosses zero at

$$V_\square = -(2/q^2)\phi_X^\perp \approx 0.201e_D. \tag{5}$$

Decreasing V below $V_\square$, the system transforms to a period-doubled phase with two molecules per rectangular unit cell (see Fig. 1) with lattice vectors $\mathbf{R}_1^{rec} = (2b,0)$ and $\mathbf{R}_2^{rec} = (0,b)$ and molecular positions $\mathbf{c}_1 = (0,u_1)$ and $\mathbf{c}_2 = (b,u_2)$ therein. Inserting these coordinates into the functional Eq. (3), we use

the Poisson summation formula replacing the real-space sum along y by the reciprocal-space sum over ℓq to obtain the energy

$$g_{pd}(\sigma,\delta) = 8\pi e_D \sum_{i,\ell > 0} \frac{\ell K_1[2\pi\ell(2i-1)]}{2i-1} \cos(q\ell\delta)$$
$$+ (V/2)[1 - \cos(q\sigma)\cos(q\delta/2)] + \text{const} \tag{6}$$

with $\sigma = (u_1 + u_2)/2$ and $\delta = (u_1 - u_2)$. The modified Bessel function $K_1(z) \propto e^{-z}$ decays rapidly and we can limit the sum in Eq. (6) to the term $i = \ell = 1$. Minimizing g_{pd} with respect to δ, we find that $\cos(q\delta/2) = (V/8\Delta)\cos(q\sigma)$ with $2\Delta = g_\square - g_\triangleright(V = 0) \approx 0.0496e_D$, and the energy reads

$$g_{pd}(\sigma) = g_\triangleright(V) - \frac{V^2}{32\Delta}\cos^2(q\sigma). \tag{7}$$

For the homogeneous period-doubled phase, $\sigma = 0$, i.e., the molecules displace symmetrically around the substrate minima along y, and $\delta = (b/\pi)\arccos(V/8\Delta)$. The condition $\delta = 0$ provides us with the critical potential $V_\square = 8\Delta \approx 0.198e_D$; this is close to the previous result (5), confirming that terms with $i > 1$ or $\ell > 1$ in Eq. (6) are indeed small. The order parameter approaches zero as $\delta \approx \pm(\sqrt{2}b/\pi)\sqrt{1 - V/V_\square}$, while $\delta = \pm b/2$ at $V = 0$ describes the *bb* lattice with energy $g_\triangleright$. The $\pm$ signs refer to the two possibilities to break the symmetry when doubling the period, leading to twin configurations with zigzag structures shifted by b along x. The period-doubled phase then exists in four versions, with the zigzag structure manifest along x or y, each with a twin shifted by b. The energy $g_{pd}(V)$ of this phase resides below the energy $g_\triangleright(V)$ of the singly locked isosceles phase (see Fig. 1).

Next, we focus our interest to weak substrate potentials V. The particle coordinates then deviate from regular triangular lattice positions, i.e., $\mathbf{R}_i^{latt} = \mathbf{R}_i^\triangle$ and $\mathbf{r}_i = \mathbf{R}_i^\triangle + \mathbf{u}_i$ in Eq. (4). For very small V, one can expand the substrate potential to linear order in the displacement [19] and minimize the correction δg in Fourier space. The force field involves the two modes $\mathbf{q}_\alpha$ of the substrate potential, folded back to the first Brillouin zone of the particle lattice, $\mathbf{q}_\alpha - n_\alpha\mathbf{K}_1 - m_\alpha\mathbf{K}_2 \equiv -\mathbf{p}_\alpha$, with $\mathbf{K}_1, \mathbf{K}_2$ the reciprocal lattice vectors of the (triangular) particle lattice, n_α, m_α are appropriate integers, and we have included a minus sign in the definition of $\mathbf{p}_\alpha$ for convenience. The minimal-energy configuration is found by rotating the triangular particle lattice with respect to the square substrate potential and relaxing the configuration in the force field. For a small misfit parameter s, one of the vectors $\mathbf{p}_\alpha$ passes near zero, generating a large deformation (and accordingly large energy gain) as the inverse elastic matrix $[\hat{\Phi}^D]^{-1}(\mathbf{k} \to 0) \propto 1/k^2$ is large at small $\mathbf{k}$. Within the resonance approximation [14,15], only the dominant term in the relaxation deriving from the small misfit vector, say $\mathbf{p}_1 = \mathbf{K}_1 - \mathbf{q}_1$, is included, while the small correction due to the other mode is dropped. Within this approximation, the optimal value of the angle φ between the symmetry axes of the particle lattice and the substrate (see Fig. 1) is given by the same formula as derived by McTague and Novaco [19] for the accommodation of a triangular lattice on a substrate with the same (triangular) symmetry but with a different lattice constant, $\varphi_s \approx \sqrt{\nu}s$. Here, $\nu = (\kappa - \mu)/(\kappa + \mu)$ is the Poisson ratio, with μ and κ the shear and compression moduli.

For the dipolar interaction $\propto R^{-3}$, one has $\nu = 9/11$ [15] [$\kappa = 10\mu$ and $\mu/n = (3/8)e_{\triangle}$] and accordingly $\varphi = 3.86°$. The energy (to leading order in s) of the distorted triangular phase reads

$$g_{\mathrm{dt}} = g_{\triangle}(V) - \frac{V^2}{64s^2}\frac{n}{\mu}(1 + \mu/\kappa) \qquad (8)$$

and we find a sinusoidal distortion field evolving along the direction $\mathbf{z} \parallel \mathbf{p}_1$ enclosing an angle $\theta = \arctan\sqrt{\nu} \approx 42.13°$ with the substrate lattice, i.e., near the diagonal.

With increasing V, this periodic distortion becomes large, of order b, and turns into a soliton array as first described by Pokrovsky and Talapov [14,15] within the same resonance approximation. Adopting a continuum elastic description and retaining the full anharmonic form of the substrate potential, they showed that the solution $\mathbf{u} = \mathbf{u}_{\mathrm{g}} + \mathbf{u}_{\mathrm{p}}$ minimizing the Gibbs free energy combines a global deformation $\mathbf{u}_{\mathrm{g}}$ with a periodic modulation $\mathbf{u}_{\mathrm{p}}$ that accounts for the soliton array. The global deformation $\mathbf{u}_{\mathrm{g}}$ involves a rotation and a uniform shear deformation, smoothly transforming the rotated triangular lattice at $V = 0^+$ into the isosceles lattice locked to the substrate along the x axis at large V. In our case, this isosceles triangular lattice (below called the bb' lattice) is characterized by a height b (along x), while in the absence of the second substrate mode, the base $b' \approx 1.0173b$ along the y axis can be found from minimizing the Gibbs free energy density $g(p)$ at fixed height b and pressure p.

The analysis of the soliton structure in Refs. [14,15] starts from the triangular lattice at small V and makes use of the associated isotropic elastic theory. Here, we focus on the first soliton entry into the bb' lattice upon decreasing V; it then is more natural to calculate the energy of the deformation $\mathbf{v}$ (defined relative to the bb' lattice) using the elastic theory of the bb' lattice, $g^{\mathrm{el}}_{bb'}(\mathbf{v}) = g_p + g_\kappa + g_\mu$, with the linear term $g_p = (\gamma_x + p)(\partial_x v_x) + (\gamma_y + p)(\partial_y v_y)$ driving the system towards the triangular phase and $g_\kappa = \kappa_x(\partial_x v_x)^2/2 + \kappa_y(\partial_y v_y)^2/2 + \kappa_{xy}(\partial_x v_x)(\partial_y v_y)$ and $g_\mu = \mu_x(\partial_y v_x)^2/2 + \mu_y(\partial_x v_y)^2/2 + \mu_{xy}(\partial_y v_x)(\partial_x v_y)$ the usual (quadratic) elastic terms [21]; the coefficients are again calculated using Ewald techniques. In this formulation, the substrate energy assumes the simple form $e^{\mathrm{sub}} = (Vn'/2)[2 - \cos(qv_x)]$ with $n' = 1/bb'$ the particle density in the bb' lattice. Aligning the rotated coordinate system $(z, z_\perp)$ with the misfit vector $\mathbf{p}_1$, the soliton displacement $\mathbf{v}(z)$ derives from a 1D sine-Gordon equation.

Using the isosceles elasticity, we find the Pokrovsky-Talapov (PT) soliton first entering the bb' lattice at $V_c^{\mathrm{PT}} \approx 0.0417e_D$; the displacement field evolves along $\theta \approx 45.05°$ ($\theta \approx 42.13°$ in the original analysis in Refs. [14,15] based on an isotropic elasticity, although see [20]) and shifts the particle lattice by $\mathbf{d} \approx (-b, 0.70b)$. With decreasing substrate amplitude V, the soliton density n_{sol} rapidly increases, $n_{\mathrm{sol}}b \propto 1/|\ln(1 - V/V_c^{\mathrm{PT}})|$; the configuration with strongly overlapping solitons at small V then is equivalent to the rotated and distorted triangular phase obtained from perturbation theory.

The soliton array obtained within the resonance approximation transforms the bb' lattice to the triangular one, while our goal here is to study the transformation of the particle system from square to triangular. The solitonic instability

then should appear on the background of the period-doubled phase, which requires us to include the second harmonic of the substrate potential into our analysis. We expect the first soliton entry in the period-doubled phase to occur at small V where we can treat the period-doubled phase as an isosceles bb lattice distorted by the relative shift $\bar{\delta} = b/2 - \delta$ of the two sublattices. Inside the soliton, the amplitude of this short-scale distortion $\bar{\delta} = (b/\pi)\arcsin[V\cos(qv_y)/8\Delta]$ is slaved to the center of mass coordinate $\mathbf{v}(\mathbf{R})$ replacing the scalar variable σ introduced above. We then have to minimize the energy

$$\delta g = \frac{1}{N}\int d^2R \left\{ g^{\mathrm{el}}_{bb}(\mathbf{v}) + \frac{Vn}{2}[1 - \cos(qv_x)] \right.$$
$$\left. + \frac{V^2 n}{64\Delta}[1 - \cos(2qv_y)] \right\}, \qquad (9)$$

where g^{el}_{bb} is the elastic Gibbs free energy [21] density of the bb lattice. While the resonance approximation admits only one low-energy soliton, the full problem with both substrate modes present allows for several line defects shifting the lattice by $\mathbf{d}_{j,k} = (-jb, kb/2)$ with j, k integers. Promising candidates reminding about the PT soliton are the $(j, k) = (1, k)$ defects, but a simple ansatz with the shift $\mathbf{d}_{01} = (0, b/2)$ should be tried as well, since the particles merely have to overcome the weak effective potential $\propto V^2/64\Delta \ll V/2$ along the y direction [see Eq. (9)]. All these line defects fall into two classes: the domain walls with $j + k$ assuming odd values and taking the period-doubled phase from one twin to the other, $\delta \to -\delta$, and the genuine solitons with $j + k$ even and the same twin on both sides, $\delta \to \delta$.

The determination of the critical substrate potential for the $(0, 1)$ domain walls is straightforward,

$$V_c^{(0,1)} = -\frac{2\pi(\gamma_y + p)}{n}\sqrt{\frac{n\Delta}{\kappa_y + \mu_y \cot^2\theta}}, \qquad (10)$$

and provides the maximal value $V_c^{(0,1)} \approx 0.0753e_D > V_c^{\mathrm{PT}}$ at $\theta = 90°$ (see Fig. 2). The analysis for the $(1, k)$ defects is more involved and the results depend strongly on the type of elasticity theory chosen for the calculation, telling us that corrections due to anharmonicities are large.
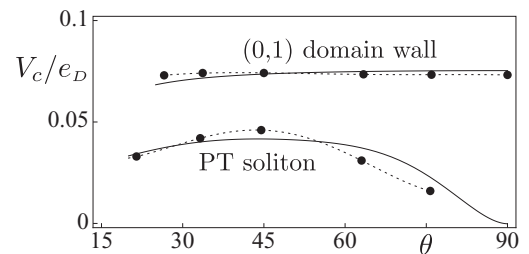

FIG. 2. Numerical results for the critical substrate potential V_c for first soliton entry versus angle θ. Shown is the data for the $(0,1)$ domain wall and for the PT soliton evaluated at selected angles defined by small Miller indices (m, n); dotted lines are guides to the eye. The flat form $V_c^{(0,1)}(\theta)$ renders the angle θ for the first $(0,1)$ domain-wall entry poorly defined. Thin lines are the analytic results following from a continuum-elastic description for an isosceles lattice.

For this reason, a reliable conclusion on the relevant scenario requires a numerically precise computation of the defects' Gibbs free energies. Starting from a variational ansatz, we relax the particle configuration numerically for periodic arrays with large separations between the defects. Summing up terms along the direction perpendicular to z reduces the problem to a 1D one, but restricts the possible angles θ to those appertaining to small Miller indices. The results for the $(0,1)$ domain wall (extrapolated to the thermodynamic limit) are shown in Fig. 2; they agree well with the analytic ones, although the largest $V_c^{(0,1)} \approx 0.074\,15e_D$ is assumed at a different angle $\theta = 45°$. While the flat dependence on angle renders the optimal orientation of the domain wall poorly defined, the data shows that the optimal defect does not align with a symmetry axis of the isosceles lattice. This result is quite unexpected, as such a symmetry alignment is predicted by the analytic calculation neglecting anharmonicities and has often been considered as natural in the literature [22]. Our numerical results [23] for the $(1,k)$ defects show that these would appear at much smaller values of V; in particular, the (second) best result $V_c^{(1,3)}(\theta = 45°) \approx 0.0544e_D$ is found for the $(1,3)$ soliton, while the $k = 2$ domain wall and $k = 1$ soliton are even worse with $V_c^{(1,2)}(45°) \approx 0.0501e_D$ and $V_c^{(1,1)}(63°) \approx 0.0382e_D$.

The proliferation of $(0,1)$ domain walls washes out the y harmonic and dilutes the particles along the y axis, thereby establishing the bb' lattice; the transformation to the (rotated) triangular lattice at $V = 0^+$ then involves an additional PT solitonic transition at lower V which smoothly eliminates the x harmonic. The analytic result for V_c^{PT} again can be improved with a numerical calculation and we find a maximal critical potential $V_c^{\mathrm{PT}}(\theta \approx 44.5°) \approx 0.046e_D$ (see Fig. 2); at this value of the substrate potential, the domain-wall phase has approached the bb' lattice to within $\approx 10\%$, as measured by the ratio of amplitudes A_p of the periodic deformation $\mathbf{v}_\mathrm{p}$ generated by the $(0,1)$ domain-wall array, $A_\mathrm{p}(V_c^{\mathrm{PT}})/A_\mathrm{p}(V_c^{(0,1)}) = 0.019/0.25 \approx 0.08$.

Depending on the specific situation at hand, alternative scenarios can be realized. All of these have to respect that a phase transition establishing an array of identical solitons with shift vector $\mathbf{d}$ [e.g., $(1,k)$ solitons or domain walls] necessarily has to be followed by a further transition at lower V; since the global distortion field in the soliton array is slaved to $\mathbf{d}$, the rotated triangular phase at $V = 0^+$ cannot be reached without the appearance of other defects. The completion of the transformation may then involve the formation of a network of crossing solitons. Furthermore, if the most favorable solitons have close critical potentials and intersect with a negative energy, the two smooth transitions can merge into a single first-order one.

To conclude, we discuss the prospects for an experimental realization and detection of these competing structures in a cold molecule system. In order to serve as a classical simulator, quantum fluctuations have to remain small. While in usual cold atom systems the latter are limited by the optical lattice, here it is the long-range interaction between the molecules that bound the zero-point motion. In estimating the importance of quantum fluctuations, we have to compare the interaction energy e_D with the recoil energy $e_\mathrm{r} = \hbar^2/mb^2$. Evaluating the quantum parameter $r_Q = e_D/e_\mathrm{r} \approx 15\,ZD[\mathrm{D}^2]/b[\mathrm{nm}]$ (with Z denoting the molecular mass and D the Debye unit) for favorable but reasonable parameter settings ($Z \sim 100$, $b \sim 500$ nm, $\sqrt{D} \sim 5$D), we obtain $r_Q \sim 10^2$. This is substantially larger than the critical value $r_Q = r_\mathrm{sf} \approx 18$ [10] marking the transition to the superfluid state where quantum fluctuations dominate [24]. Hence molecular systems can serve as classical simulators, although some renormalization effects due to quantum fluctuations may occur. Furthermore, sufficiently large amplitudes V must be reached for the optical lattice; in a recent experiment [25], dipolar molecules have been localized in deep wells $V \sim 10^2 e_\mathrm{r}$, which should be sufficient to reach the critical value $V_\square$. Finally, a promising way to identify the various structural phases is via their different dynamical response under an applied force field $\mathbf{f}$, with the square and period-doubled phases characterized by symmetric and asymmetric (reduced along y) pinning, respectively. For practical purposes, the exponentially weak pinning of solitons can be neglected; the force field $\mathbf{f}$ induces a drive $\mathbf{f} \cdot \mathbf{d}_{j,k}$ along z and the resulting soliton motion generates a mass flow along $\mathbf{d}_{j,k}$ which allows one to identify the two solitonic phases.

[1] E. D. Specht, M. Sutton, R. J. Birgeneau, D. E. Moncton, and P. M. Horn, Phys. Rev. B **30**, 1589 (1984); R. J. Birgeneau and P. M. Horn, Science **232**, 329 (1986).

[2] O. Daldini, P. Martinoli, J. L. Olsen, and G. Berner, Phys. Rev. Lett. **32**, 218 (1974); A. T. Fiory, A. F. Hebard, and S. Somekh, Appl. Phys. Lett. **32**, 73 (1978).

[3] K. Harada, O. Kamimura, H. Kasai, T. Matsuda, A. Tonomura, and V. V. Moshchalkov, Science **274**, 1167 (1996).

[4] J. W. Reijnders and R. A. Duine, Phys. Rev. Lett. **93**, 060401 (2004).

[5] R. A. Webb, R. F. Voss, G. Grinstein, and P. M. Horn, Phys. Rev. Lett. **51**, 690 (1983); Ch. Leemann, Ph. Lerch, G. A. Racine, and P. Martinoli, *ibid.* **56**, 1291 (1986).

[6] K. Mangold, P. Leiderer, and C. Bechinger, Phys. Rev. Lett. **90**, 158302 (2003).

[7] J. Doyle, B. Friedrich, R. V. Krems, and F. Masnou-Seeuws, Eur. Phys. J. D **31**, 149 (2004).

[8] D. Wang, J. Qi, M. F. Stone, O. Nikolayeva, H. Wang, B. Hattaway, S. D. Gensemer, P. L. Gould, E. E. Eyler, and W. C. Stwalley, Phys. Rev. Lett. **93**, 243005 (2004).

[9] J. M. Sage, S. Sainis, T. Bergeman, and D. DeMille, Phys. Rev. Lett. **94**, 203001 (2005).

[10] H. P. Büchler, E. Demler, M. Lukin, A. Micheli, N. Prokof'ev, G. Pupillo, and P. Zoller, Phys. Rev. Lett. **98**, 060404 (2007).

[11] Y. I. Frenkel and T. Kontorowa, Zh. Eksp. Teor. Fiz. **8**, 1340 (1938).

[12] F. C. Frank and J. H. Van der Merwe, Proc. R. Soc. **198**, 205 (1949).

[13] V. L. Pokrovsky and A. L. Talapov, Phys. Rev. Lett. **42**, 65 (1979).

[14] V. L. Pokrovskii and A. L. Talapov, Zh. Eksp. Teor. Fiz. **78**, 269 (1980) [Sov. Phys. JETP **51**, 134 (1980)].

[15] V. L. Pokrovsky and A. L. Talapov, *Theory of Incommensurate Crystals* (Harwood, Chur, 1984).

[16] P. P. Ewald, Ann. Phys. (Leipzig) **64**, 253 (1921).

[17] W. V. Pogosov, A. L. Rakhmanov, and V. V. Moshchalkov, Phys. Rev. B **67**, 014532 (2003).

[18] V. Zhuravlev and T. Maniv, Phys. Rev. B **68**, 174507 (2003).

[19] J. P. McTague and A. D. Novaco, Phys. Rev. B **19**, 5299 (1979).

[20] In Ref. [14] the Poisson ratio was mistakenly evaluated to $\nu = 5/11$ producing an angle $\theta \approx 24°$ (corrected in Ref. [15]).

[21] We include here a term $p\,\delta A/A$.

[22] J. Villain, in *Ordering in Two Dimensions*, edited by S. Sinha (North-Holland, New York, 1980); P. M. Chaikin and T. C. Lubensky, *Principles of Condensed Matter Physics* (Cambridge University Press, Cambridge, 1995).

[23] B. Gränz, S. E. Korshunov, V. B. Geshkenbein, and G. Blatter (unpublished).

[24] Exploiting the large dipole moment $\sqrt{D} = 8.9$ D [26] of SrO and using $b \sim 300$ nm one can reach $r_Q \sim 400$ [10].

[25] A. Chotia, B. Neyenhuis, S. A. Moses, Bo Yan, J. P. Covey, M. Foss-Feig, A. M. Rey, D. S. Jin, and Jun Ye, Phys. Rev. Lett. **108**, 080405 (2012).

[26] M. Kaufmann, L. Wharton, and W. Klempere, J. Chem. Phys. **43**, 943 (1965).